The Influence of Dislocation Substructure on Creep Rate during Accelerating Creep Stage of Single Crystal Nickel-based Superalloy, CMSX-4

Nobuhiro Miura, Yoshihiro Kondo and Narihito Ohi*
The National Defense Academy, Yokosuka 239-8686, Japan
*Ishikawajima-Harima Heavy Industries Co., Ltd. Tokyo 188-8555, Japan

Abstract

The evolution of the dislocation substructure during the accelerating creep stage in the single crystal nickel-based superalloy, CMSX-4, was investigated through the microstructural observation of interrupted creep specimens at 1273K-160MPa. The dislocation substructure evolved, not within γ', but at the γ/γ' interface and in the γ channel. The dislocation density at the γ/γ' interface increased with increasing creep deformation. The correlation between the dislocation density and the creep rate during the accelerating creep stage led to an equation relating the creep rate to the fifth power of the dislocation density. This result was quite different from the supposition proposed by Dyson et al. that the creep rate during the accelerating creep stage would be directly proportional to the dislocation density. They supposed that the dislocations at the γ/γ' interface acted as mobile ones. The thickness of the γ channel increased with creep, and the creep rate during the accelerating creep stage was proportional to the fifth power of the thickness of the γ channel. The increase in the thickness of the γ channel meant the increase in the radius of dislocation curvature in the γ channel, then the loss of creep resistance during the accelerating creep stage would be interpreted by an increase in the radius of dislocation curvature. This same correlation between the creep rate during the accelerating creep stage and the thickness of the γ channel at 160MPa was confirmed in the wide stress range of 100 to 400MPa. Using the creep rate-γ channel thickness curves, the creep rate at the certain thickness of the γ channel were estimated, and the stress-creep rate curve at the certain thickness of the γ channel could be drawn. Comparing the measured stress-creep rate curve with the estimated stress-creep rate curve (at the certain thickness of the γ channel), the lager creep rate was obtained at a lower stress level, and this was also interpreted by an increase in the thickness of the γ channel. Consequently, the present experimental evidence, showing the effect of the thickness of the γ channel on the creep rate was confirmed.

Superalloys 2000
Edited by T.M. Pollock, R.D. Kissinger, R.R. Bowman,
K.A. Green, M. McLean, S. Olson, and J.J. Schirra
TMS (The Minerals, Metals & Materials Society), 2000

Introduction

Kondo et al. compared the creep rate of prior-creep tested specimens of the single crystal nickel-based superalloy, CMSX-4, with that of the as-heat treated one, using a stress-enhanced creep test[1)-4)]. Stress-enhanced creep tests were conducted at 1273K-250MPa, using the specimen interrupted prior-creep tests at 1273K-160MPa in the wide creep range from the transient to the accelerating creep stage. The microstructural observations were done for creep interrupted specimens and the rafting process was examined. And it was indicated that the rafting of the γ' phase acted as a creep weakener and that the loss of creep resistance was caused by the widening of the γ channel. The extending of the γ channel led to an increase in the radius of dislocation curvature in the γ channel. This supposition was substantially accepted to interpret the accelerating creep. However, it is important to directly investigate the correlation between the thickness of the γ channel and the creep rate during the accelerating creep stage.

This study was undertaken to show that the origin of the onset of the accelerating creep in the single crystal nickel-based superalloy was caused not by mechanical damage like voids and cracks, but by microstructural changes. Dyson et al. also indicated that the onset of the accelerating creep in the nickel-based superalloy was caused by a microstructural change, that is, an increase in the dislocation density at the γ/γ' interface[5)]. They determined the dislocation at the γ/γ' interface acted as the mobile dislocation, so an increase in the dislocation density meant an increase in the creep rate according to the Orowan equation of $\dot{\varepsilon} = \rho b v$, where $\dot{\varepsilon}$ is the creep rate, ρ is the dislocation density, b is the burgers vector and v is the velocity of the dislocation. This conception was based on the dislocation glide model. In contrast to the model proposed by Dyson et al., the supposition proposed by Kondo et al. was based on the dislocation climb model.

Experimental procedure

A single crystal alloy of CMSX-4 (having the chemical composition in weight percent ; 6.4Cr, 9.3Co, 5.5Al, 0.9Ti, 6.3Mo, 6.2Ta, 6.2W, 2.8Re, 0.1Hf, balance Ni) was prepared in the form of bars 13mm in diameter by a directional precision casting. The exact orientations were determined by the Laue back-reflection technique ; longitudinal axes of single crystals selected for this study were within 5deg of the [001] orientation. After employing an eight step solution treatment (1550Kx7.2ks → 1561Kx7.2ks → 1569Kx10.8ks → 1577x10.8ks → 1586Kx7.2ks → 1589Kx7.2ks → 1591Kx7.2ks → 1594Kx7.2ks → GFC) and a three step aging heat treatment (1413Kx21.6ks → 1353Kx21.6ks → 1144Kx72ks → AC), the specimens for the creep tests with a gauge diameter of 6mm and a gauge length of 30mm were prepared.

The creep tests were carried out at 1273K-160MPa (creep rupture life is 3.60×10^6s) under constant load. Creep strain was measured automatically through linear variable differential transformers (LVDT's) attached to extensometers. The creep tests were interrupted at the certain times ranging from the transient creep stage to the accelerating creep stage. All the creep interrupted specimens were followed by cooling under load.

Microstructural examinations by a scanning electron microscopy (SEM ; Hitachi S-4200) and by a transmission one (TEM ; Hitachi H-8000) were carried out on the specimens sectioned parallel to (100), (101) and (111) planes. Specimens for the SEM observation were prepared metallographically and electroetched with a supersaturated phosphoric acid-chromic acid solution. TEM foils were electropolished with a 5% solution of perchloric acid in alcohol. The thickness of the γ channel was measured by use of the image processor-analyzer.

Results

Microstructure of the as-heat treated specimen

The microstructure of the as-heat treated CMSX-4 is shown in Fig. 1. The cuboidal γ' phase is regularly arrayed in the γ matrix. The average edge length of the cuboidal γ' phase is

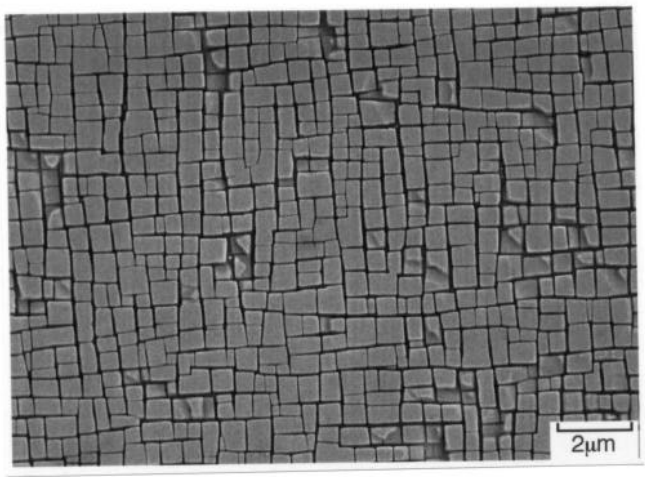

Fig. 1. Scanning electron micrograph of a single crystal nickel-based superalloy, CMSX-4.

about 0.5μm. The mean thickness of the γ channel is approximately 0.1μm. The volume fraction of the γ' phase is about 80 percent. There were no eutectic γ' phase.

Creep interrupted test

The creep rate-time curve of CMSX-4 at 1273K-160MPa is shown in Fig. 2. As described in the previous reports[1)-3)], the creep curve at 1273K-160MPa consists of the transient creep stage and the accelerating creep stage. The conception that creep in single crystal nickel-based superalloys consisted of the extended steady state and the accelerating creep stage and the ratio of the transient creep stage to rupture life was small, was perfectly disappeared. In this case, the ratio of the transient creep stage to rupture life occupied more than 10 percent. The open circles corresponded to time where the creep tests were interrupted to prepare the specimens for the microstructural examinations. Creep interrupted tests were done over a wide range from the latter half of the transient creep stage to the end of the accelerating creep stage.

Microstructural changes during creep

The scanning electron micrographs of the specimens tested for $1.08x10^5$, $1.08x10^6$ and $3.24x10^6$s are shown in Fig. 3. The stress axis was the normal direction of these photos. By subjecting the creep testing time of $1.08x10^5$s (Fig. 3a), at the latter half of the transient creep stage, the γ' phase is remained cuboidal, whereas some of the cuboidal γ' phase contact each other. After connecting to each other, the lamellar γ/γ' structures, that is, rafted γ' structures, form

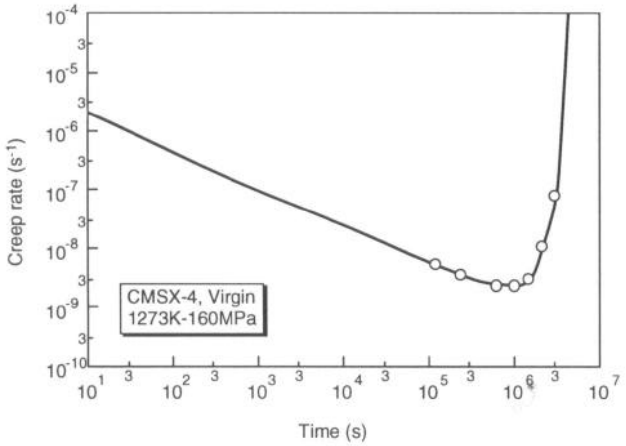

Fig. 2. Creep rate-time curve of CMSX-4 at 1273K-160MPa. The open circles correspond to time where the creep tests were interrupted for the microstructural examinations.

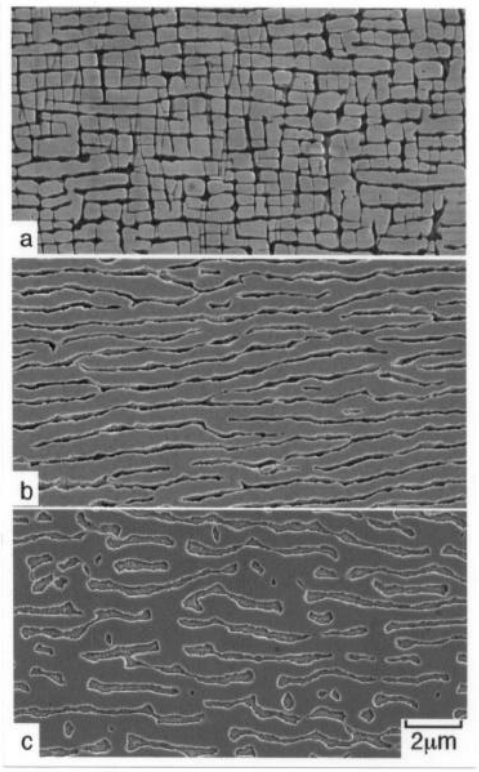

Fig. 3. Scanning electron micrographs of the specimens tested at 1273K-160MPa for (a) $1.08x10^5$, (b) $1.08x10^6$ and (c) $3.24x10^6$s. Stress axis is vertical in these photos.

perpendicular to the stress axis as shown in Fig. 3b (the specimen creep tested for $1.08x10^6$s). Further coarsening of the γ' phase is detected in the specimen tested for $3.24x10^6$s (Fig. 3c), at the end of the accelerating creep stage. Regularity of the rafted γ' diminishes.

The transmission electron micrograph of the specimen tested for $1.08x10^5$s, at the end of the transient creep stage, is shown in Fig. 4, where the electron beam direction, B,

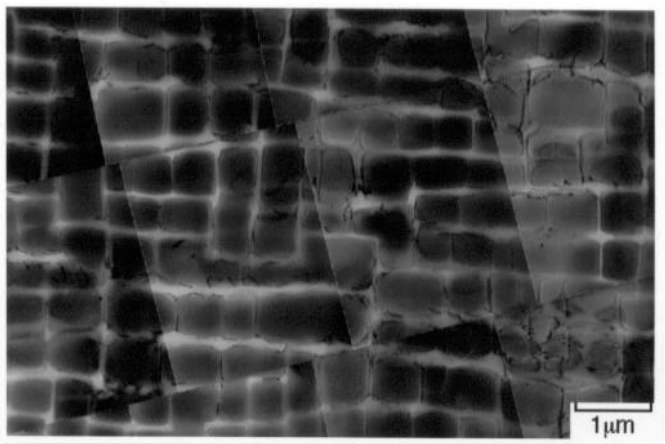

Fig. 4. Transmission electron micrograph of the specimen tested at 1273K-160MPa for $1.08x10^5$s, where B=[100]. Stress axis is vertical in this photo.

was close to [100]. Few dislocations are observed in the γ matrix and the γ' phase, while a small number of dislocations are present at the γ/γ' interface.

For the specimen tested for $1.08x10^6$s, at the minimum creep rate, Fig. 5, where B=[100], few dislocations are observed in the γ matrix and the γ' phase, similar to the specimen tested for $1.08x10^5$s. However, a number of dislocations are observed at the γ/γ' interface.

For the specimen tested for $3.24x10^6$s, at the end of the accelerating creep stage, Fig. 6, where B=[100], few dislocations are observed in the γ matrix and the γ' phase, similar to the specimens creep tested for $1.08x10^5$ and $1.08x10^6$s. A large number of dislocations are observed at the γ/γ' interface.

Thus few dislocations existed within the γ' phase and there was no evidence that the dislocations cut through the γ' phase. The dislocation density at the γ/γ' interface was found to increase with increasing creep deformation. However, TEM observation where B=[100] did not indicate accurate information about the dislocation substructure, such as the dislocation density, at the γ/γ' interface. Consequently, it was necessary to carry out TEM observations where B=[101].

The transmission electron micrograph of the specimen tested for $1.08x10^5$s, at the latter half of the transient creep stage, is shown in Fig. 7, where B=[101]. A few dislocations are observed at the γ/γ' interface.

In the specimen tested for $1.08x10^6$s, at the minimum creep rate, Fig. 8, where B=[101], most of the dislocations are aligned. The dislocation density at the γ/γ' interface is higher than that of the specimen tested for $1.08x10^5$s (Fig. 7).

In the specimen tested for $3.24x10^6$s, at the end of the accelerating creep stage, Fig. 9, where B=[101], the dislocations are tangled with each other. The dislocation density at the γ/γ' interface is considerably higher than that

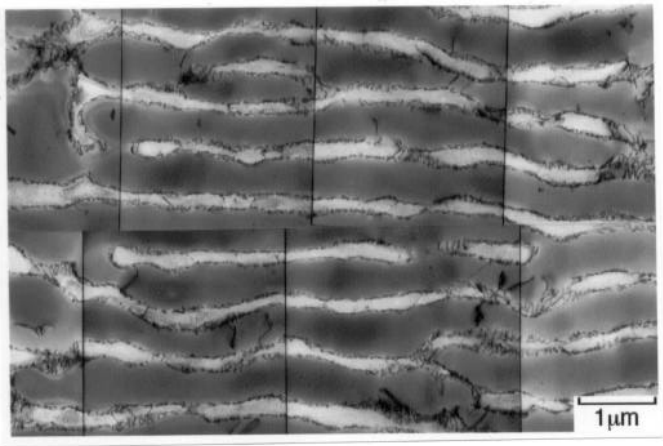

Fig. 5. Transmission electron micrograph of the specimen tested at 1273K-160MPa for $1.08x10^6$s, where B=[100]. Stress axis is vertical in this photo.

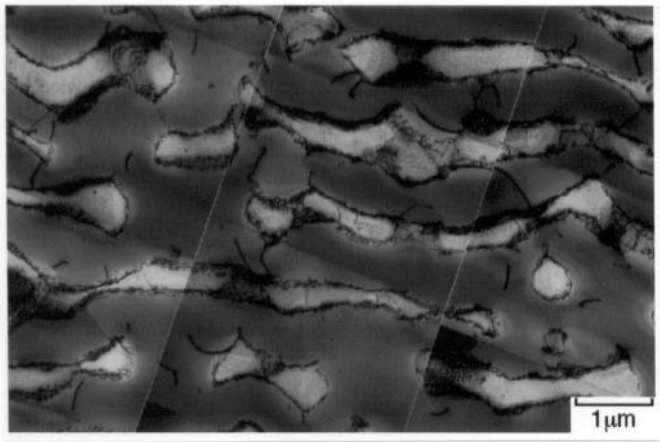

Fig. 6. Transmission electron micrograph of the specimen tested at 1273K-160MPa for $3.24x10^6$s, where B=[100].

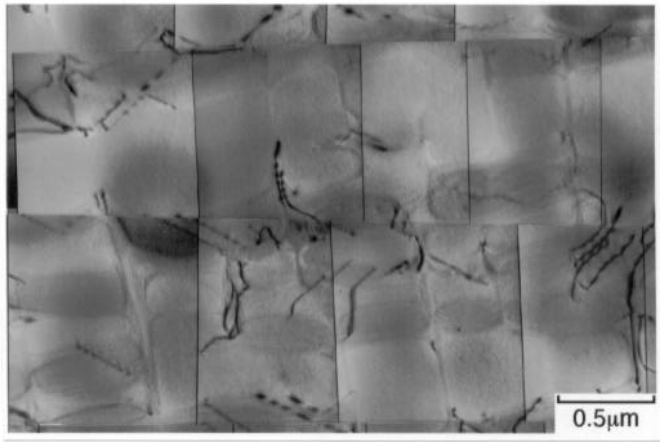

Fig. 7. Transmission electron micrograph of the specimen tested at 1273K-160MPa for $1.08x10^5$s, where B=[101].

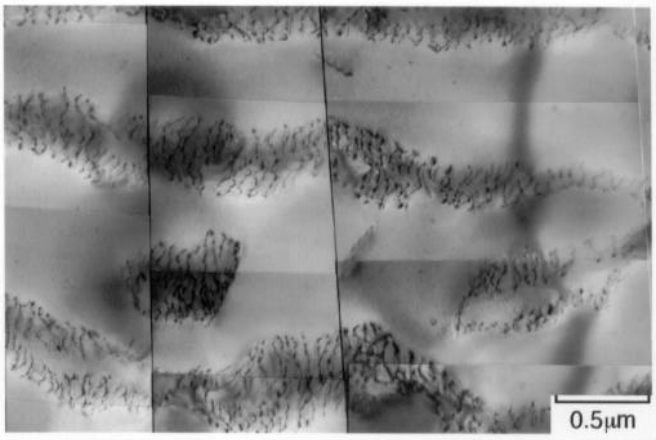

Fig. 8. Transmission electron micrograph of the specimen tested at 1273K-160MPa for $1.08x10^6$s, where B=[101].

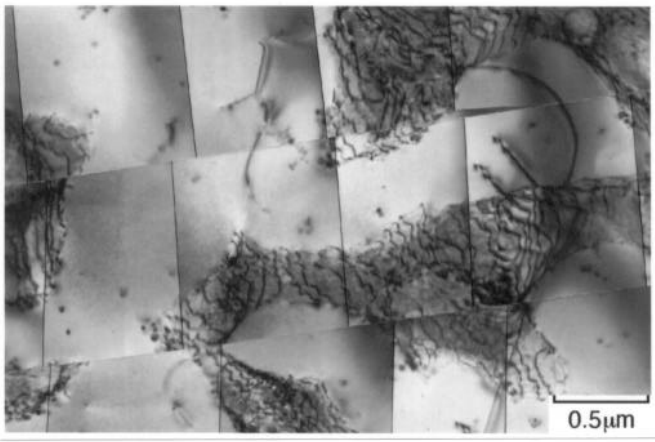

Fig. 9. Transmission electron micrograph of the specimen tested at 1273K-160MPa for 3.24×10^6s, where B=[101].

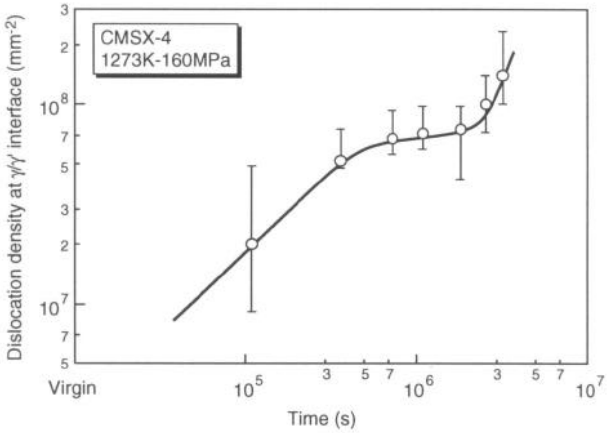

Fig. 10. Change in the dislocation density at the γ/γ' interface with the creep time.

of the other specimens, and therefore, increased remarkably with increasing creep deformation.

Discussion

Dyson et al. suggested that the rate-controlling process of the creep deformation of the nickel-based superalloys was the dislocation glide, since an increase in the creep rate during the accelerating creep stage was interpreted by an increase in the mobile dislocation density as mentioned before[5]. In the present study, attention is paid to the dislocation density at the γ/γ' interface which changed remarkably during creep deformation. One more important point is that the dislocation density at the γ/γ' interface was measured quantitatively on the specimens selected parallel to (101) planes, according to the Hirsch's manner[6], thereby more detailed observations could be done in order to evaluate the suggestion proposed by Dyson et al.

The change in the dislocation density at the γ/γ' interface with the creep testing time is shown in Fig. 10. The dislocation density increased after subjecting creep tests up to 3×10^5s, and leveled off at 7×10^7mm^{-2} at 10^6s. However, with further increasing time, the dislocation density increased markedly, corresponded to an increase in the creep rate during the accelerating creep stage, Fig. 2.

The creep rate during just the accelerating creep stage was plotted as a function of the dislocation density at the γ/γ' interface, as indicated in Fig. 11. The correlation between the creep rate during the accelerating creep stage and the dislocation density at the γ/γ' interface showed linear behavior on a log-log scale, the slope being five. In case that the creep rate was controlled by the dislocation glide suggested by Dyson et al., the linear slope would be one.

Consequently, it is difficult to state that the increase in the creep rate during the accelerating creep stage results from an increase in the dislocation density at the γ/γ' interface. In general, an increase in the creep rate during the accelerating creep stage of the polycrystalline heat-resistant alloys has been thought to be mainly attributable to the stress increase by the reduction of the cross-sectional area due to mechanical damage such as initiation and propagation of cracks[7][8]. However, no cracks and voids were

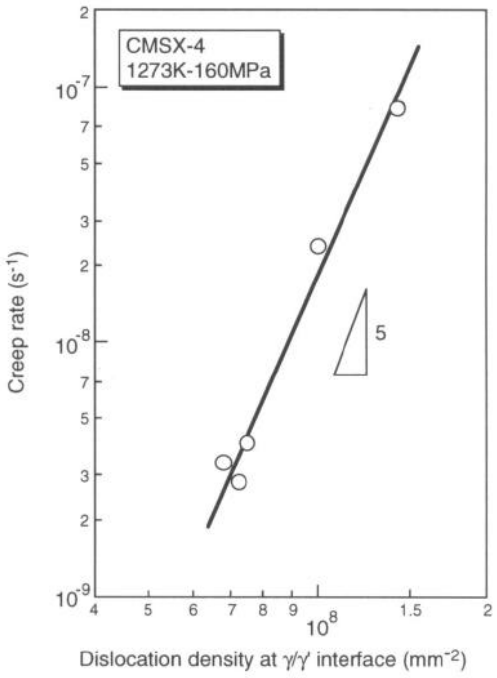

Fig. 11. Relation between the creep rate during the accelerating creep stage and the dislocation density at the γ/γ' interface.

observed even in the scanning electron micrograph of the specimen tested for $3.24x10^6$s, at the end of the accelerating creep stage (Fig. 3c). Therefore, it was difficult to claim that the creep rate during accelerating creep stage of this single crystal nickel-based superalloy was attributable to the stress increase due to mechanical damage. On the other hand, it was reported that an increase in the creep rate during the accelerating creep stage of the polycrystalline heat-resistant alloys was caused by the loss of creep resistance through the microstructural changes[9)-18)].

Kondo et al. revealed that the minimum creep rate of the single crystal nickel-based superalloy directly correlated with the radius of dislocation curvature which was the reflection of the thickness of the γ channel, independent of the shape and the size of γ' phase[1)]. Then, the change in the thickness of the γ channel with creep deformation was examined. From the SEM observation of the specimens tested for $1.08x10^5$, $1.08x10^6$ and $3.24x10^6$s as shown in Fig. 3, the thickness of the γ channel seemed to increase with an increase in the creep testing time.

The thickness of the γ channel of the interrupted specimens was plotted as a function of the creep testing time as shown in Fig. 12. The thickness of the γ channel increased immediately after loading and increased markedly after 10^6s, when γ' phase rafting occurred. This increase in the γ channel corresponded to the increase in the creep rate during the accelerating creep stage, Fig. 2.

The creep rate during the accelerating creep stage was plotted as a function of the thickness of the γ channel in Fig. 13. The correlation between the creep rate during the accelerating creep stage and the thickness of the γ channel was linear on a log-log scale, the slope being five. Consequently, an increase in the creep rate during the accelerating creep stage was caused by the loss of creep resistance through an increase in the thickness of the γ channel.

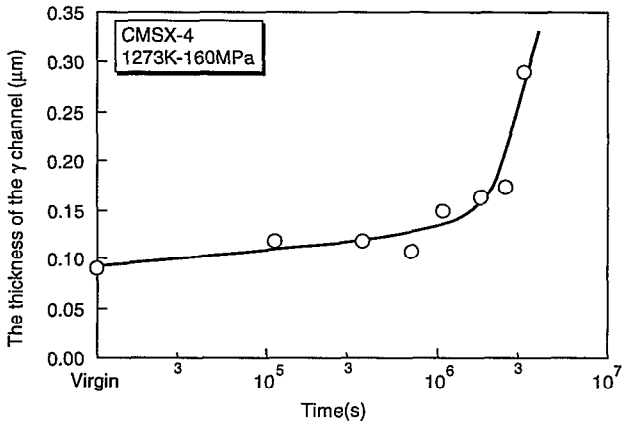

Fig. 12. Change in the thickness of the γ channel of the interrupted specimens with the creep time.

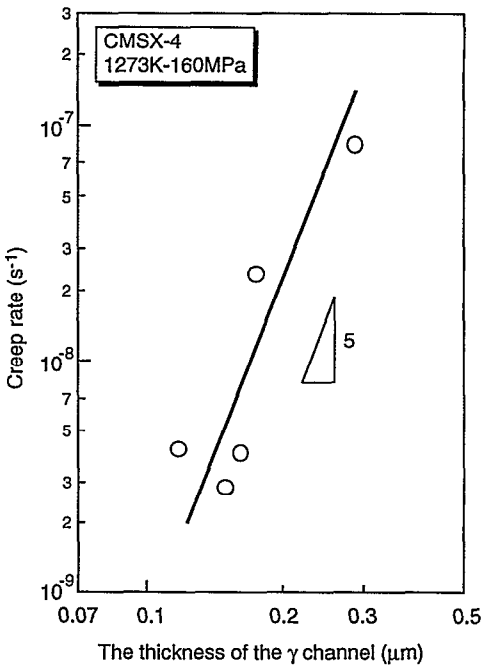

Fig. 13. Relation between the creep rate during the accelerating creep stage and the thickness of the γ channel of the interrupted specimens.

High magnification transmission electron micrographs of the specimens creep tested for $1.08x10^5$, $1.08x10^6$ and $3.24x10^6$s was shown in Fig. 14, where B=[100]. The bent dislocation with the small radius of curvature was observed within the γ channel of the specimen creep tested for $1.08x10^5$s (Fig. 14a), at the latter half of the transient creep stage. The radius of dislocation curvature of the specimen creep tested for $1.08x10^6$s (Fig. 14b), at the minimum creep rate, was larger than that of the specimen creep tested for $1.08x10^5$s and smaller than that of the specimen creep tested for $3.24x10^6$s (Fig. 14c), at the end of the accelerating creep stage. The radius of dislocation curvature of these specimens cannot be quantitatively compared with that of the other specimens because the electron beam direction was not perpendicular to (111) planes which were the slip plane of FCC metals. But the radius of dislocation curvature seemed to increase with increasing the creep testing time. Here, the radius of dislocation curvature, R_d, is inversely proportional to the shear stress, $\tau = A/R_d$ (A ; constant), therefore the smaller radius of dislocation curvature resists a larger shear stress[19)-21)]. Conversely, an increase in the radius of dislocation curvature facilitates dislocation motion. The measurements of the radius of dislocation curvature

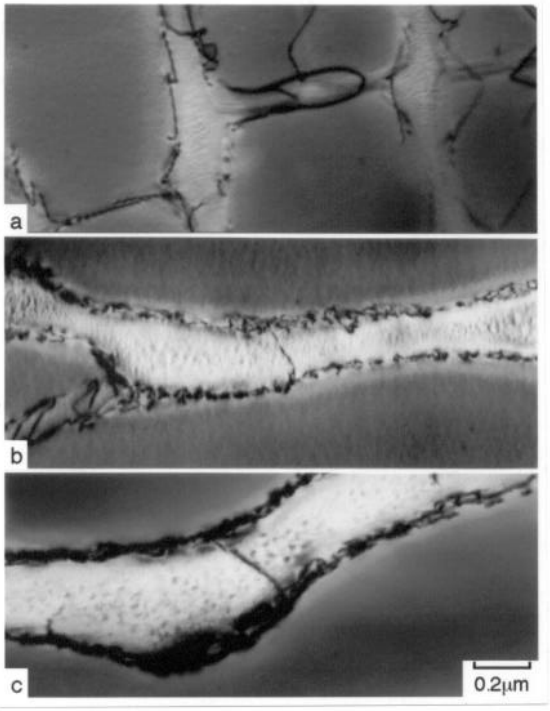

Fig. 14. High magnification transmission electron micrographs of the specimens tested at 1273K-160MPa for (a) 1.08×10^5, (b) 1.08×10^6 and (c) 3.24×10^6s. Stress axis is vertical in these photos.

were made on the specimens sectioned parallel to (111) planes which are the slip planes of FCC metals.

The relationship between the radius of dislocation curvature and the thickness of the γ channel was shown in Fig. 15, where the thickness of the γ channel was converted to the spacing between the two neighboring γ' phases on (111) planes. The radius of dislocation curvature was directly proportional to the thickness of the γ channel. From these results, it was concluded that an increase in the creep rate during the accelerating creep stage was caused by the loss of creep resistance through an increase in the radius of dislocation curvature.

Kondo et al. examined the stress exponent of the minimum creep rate, n-value, of the single crystal nickel-based superalloy, CMSX-4, crept at 1273K in the stress range of 100 to 400MPa, and suggested that a decrease in n-value from 7 at the high stress level to 3 at the low stress level resulted from a decrease in creep resistance due to the formation of the rafted structure of γ' phases[4)22)23)]. In this wide stress range, creep rate of the single crystal nickel-based superalloy may be expected to be dependent upon the thickness of the γ channel. Therefore, the thickness of the γ channel of CMSX-4 was measured on the creep interrupted specimens used in previous works[1)-4),22)-27)].

The minimum creep rate and the creep rate during the accelerating creep stage were used as the creep rate. The data at 1273K for the range of 100 to 400MPa was plotted as a function of the thickness of the γ channel in Fig. 16.

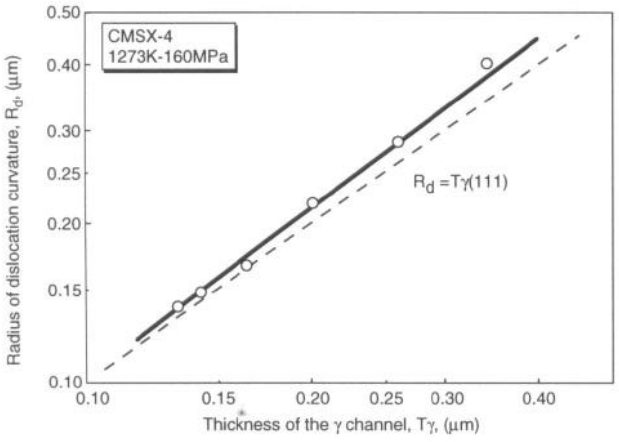

Fig. 15. Relation between the radius of dislocation curvature and the thickness of the γ channel of the interrupted specimens.

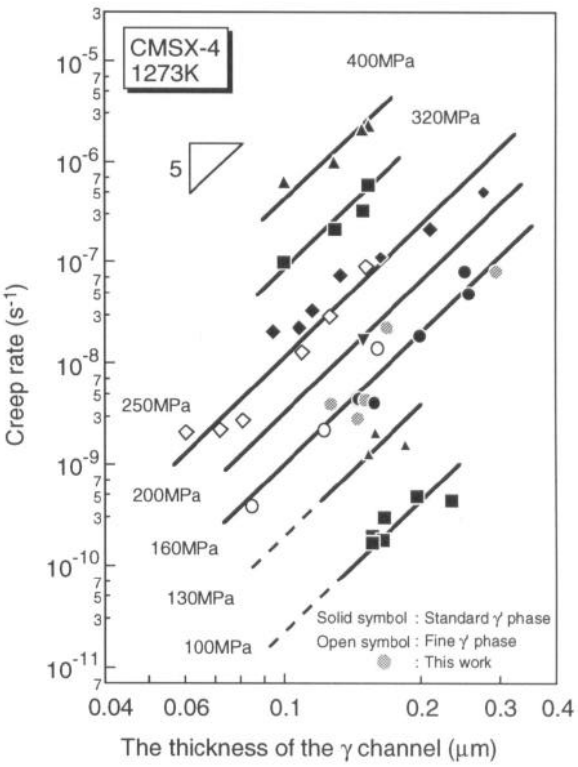

Fig. 16. Relation between creep resistance, that is, the minimum creep rate and the creep rate during the accelerating creep stage, and the thickness of the γ channel of CMSX-4 crept at 1273K in the stress range from 100 to 400MPa.

The correlation between the creep rate and the thickness of the γ channel was linear on a log-log scale; the curves at the stresses of 400, 320, 250, 160 and 100MPa have the same slope of five. The curves with the slope of five were drawn at 130 and 200MPa.

From seven straight lines in Fig. 16, stress-creep rate curve under the constant thickness of the γ channel could be drawn, as shown in Fig. 17. The solid line was the estimated one at the thickness of the γ channel of 0.1μm, which was the initial thickness of the γ channel. As shown in Fig. 17, the solid line was bent at the stress of 250MPa. Under the stresses less than 250MPa where the cuboidal γ' phase turned to the rafted structure, the solid line had the slope with the value of five. For the stresses larger than 250MPa, the cuboidal γ' phase remained at the minimum creep rate. The estimated stress-creep rate curve was compared with the measured one, the dotted line. The estimated creep rate was smaller than the measured one under the stresses less than 250MPa. In this case, the rafted γ' structures acted as a creep weakener, whereas the measured creep rate was approximately equal to the calculated one at the higher stresses than 250MPa where the γ' phase remained cuboidal. From these results, it was concluded that an increase in the creep rate at the lower stresses caused by an increase in the thickness of the γ channel due to the γ' phase rafting.

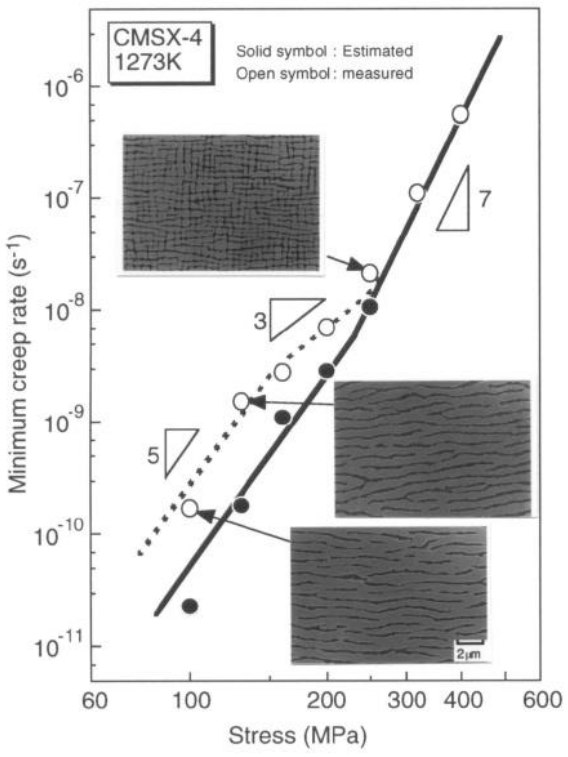

Fig. 17. Estimated and measured stress-minimum creep rate curves of CMSX-4 at 1273K.

Conclusions

Creep resistance, especially the creep rate during the accelerating creep stage crept at 1273K-160MPa, of the single crystal nickel-based superalloy, CMSX-4, was investigated in connection with the dislocation substructure. The results can be summarized in the following.

1) The γ/γ' lamellar structures were formed perpendicular to the stress axis at the minimum creep rate, but regularity of the rafted γ' diminished at the accelerating creep stage.

2) The dislocation substructure was not formed in the γ' phase, and the dislocation density at the γ/γ' interface increased with the creep deformation.

3) The correlation between the creep rate during the accelerating creep stage and the dislocation density at the γ/γ' interface was linear on a log-log scale, the slope being five. The slope was different from the supposition proposed by Dyson et al., that an increase in the creep rate during the accelerating creep stage resulted from an increase in the mobile dislocation density.

4) The thickness of the γ channel increased with creep deformation and the correlation between the thickness of the γ channel and the creep rate during the accelerating creep stage was linear.

5) The radius of dislocation curvature was directly proportional to the thickness of the γ channel.

6) Consequently, an increase in the creep rate during the accelerating creep stage was attributable to the loss of creep resistance due to an increase in the radius of dislocation curvature caused by an increase in the thickness of the γ channel.

7) The correlation between creep resistance, $\dot{\varepsilon}$, and the thickness of the γ channel, t_γ, of the single crystal nickel-based superalloy, CMSX-4, crept at 1273K in the stress range from 100 to 400MPa showed $\dot{\varepsilon} \quad t_\gamma^5$ behavior.

8) Comparing the practical stress-creep rate curve with the estimated stress-creep rate curve at the certain thickness of the γ channel, the estimated creep rate was smaller than the measured one under the stresses less than 250MPa where the cuboidal γ' phase turned to the rafted structure.

9) From these results, it was concluded that an increase in the creep rate at the lower stresses caused by an increase in the thickness of the γ channel due to the γ' phase rafting.

Reference

1) Y. Kondo et al., "Effect of Morphology of γ' Phase on Creep Resistance of A Single Crystal Nickel-Based Superalloy, CMSX-4," Proc. of the 8th Inter. Conf. Superalloys '96,

(1996), 297-304.
2) N. Kitazaki et al., "Effect of Aging and Stress Aging on Creep Resistance of Single Crystal Ni-base Superalloy, CMSX-4," 123rd Committee on Heat Resisting Metals and Alloys Rep., 34 (1993), 173-181.
3) Y. Kondo et al., "Effect of Aging and Stress Aging on Creep Resistance of Single Crystal Ni-base Superalloy CMSX-4," Tetsu-to-Hagané, 80 (1994), 568-573.
4) Y. Kondo and T. Matsuo, "Creep of Single Crystal Superalloys," 123rd Committee on Heat Resisting Metals and Alloys Rep., 38 (1997), 269-286.
5) B. F. Dyson and M. McLean, "Particle-coarsening, σ_0 and Tertiary Creep" Acta Metall., 31 (1983), 17-27.
6) P. B. Hirsch et al., Electron Microscopy of Thin Crystals (London: Butterworths, 1965), 422.
7) D. A. Woodford, "Creep Damage and the Remaining Life Concept," J. Eng. Mater. Technol., 101 (1979), 311-316.
8) N. Shin-ya and S. R. Keown, "Correlation between Rupture Ductility and Cavitation in Cr-Mo-V Steels," Mater. Sci., 13 (1979), 89-93.
9) K. R. Williams and B Wilshire, "Effect of Microstructural Instability on the Creep and Fracture Behavior of Ferritic Steels," Mater. Sci. Eng., 28 (1977), 289-296.
10) K. R. Williams and B Wilshire, "Creep behavior of 1/2Cr 1/2Mo 1/4V Steel at Engineering Stresses," Mater. Sci. Eng., 38 (1979), 199-210.
11) C. N. Bolton, B. F. Dyson and K. R. Williams, "Metallographic Methods of Determining Residual Creep Life," Mater. Sci. Eng., 46 (1980), 231-239.
12)L. P. Stoter, "Thermal Aging Effects in AISI Type 316 Stainless Steel," J. Mater. Sci., 16 (1981) 1039-1051.
13) R. A. Stevens and P. E. J. Flewitt, "The Effects of γ' Precipitate Coarsening During Isothermal Aging and Creep of the Nickel-base Superalloy IN-738," Mater. Sci. Eng., 37 (1979), p.237-247.
14) J. M. Leitnaker and J. Bentley, "Precipitate Phases in Type 321 Stainless Steel after Aging 17 Years at ~ 600℃," Metall. Trans. A, 8 (1977), 1605-1613.
15) J. H. Hoke and F. Eberle, "Experimental Superheater for Steam at 2000Psi and 1250 F - Report after 14,281 Hours of Operation," Trans. ASME, 79 (1957), 307-317.
16) M. Tanaka et al., "Study on Microstructure and Mechanical Properties of SUS 304 Used for a Long Time at Elevated Temperature," 123rd Committee on Heat Resisting Metals and Alloys Rep., 24 (1983), 373-384.
17) Y. Kondo et al., "Effect of Recovery Treatment on the Mechanical Properties of SUS 304 Serviced for Prolong Time at Elevated Temperature," 123rd Committee on Heat Resisting Metals and Alloys Rep., 26 (1985), 133-139.
18) Y. Yamaguchi et al., "Microstructures and Mechanical Properties of SUS304 Serviced for Prolonged Time at 520 ~ 610℃," Tetsu-to-Hagané, 24 (1984), B-61
19) A. Kelly and R. B. Nicholson, Strengthening Methods in Crystals (Amsterdam: Elsevier, 1971),9.
20) F. R. N. Nabarro, Theory of Crystal Dislocations (London: Oxford, 1967), 53.
21) J. Weertman and J. R. Weertman, Elementary Dislocation Theory (New York, NY: Macmillan, 1964)
22) N. Kitazaki et al., "Creep Resistance of Single Crystal Ni-base Superalloy, CMSX-4, at 1273K," 123rd Committee on Heat Resisting Metals and Alloys Rep., 35 (1994), 353-360.
23) K. Ishibashi et al., "Long-term Creep Rupture Properties of Single Crystal Ni-base Superalloy, CMSX-4," 123rd Committee on Heat Resisting Metals and Alloys Rep., 37 (1996), 1-10.
24) N. Kitazaki et al., "Applied Stress Dependence of Transient Creep in Single Crystal Ni-based Superalloy," CAMP ISIJ, 7 (1994), 739.
25) N. Kitazaki et al., "Creep Resistance of Single Crystal Ni-based Superalloy, CMSX-4 at 1273K," CAMP ISIJ, 6 (1993), 1725.
26) Y. Hoshizashi et al., "Change in the Radius of Dislocation Curvature with Creep Deformation in Single Crystal Ni-base Superalloy, CMSX-4," 123rd Committee on Heat Resisting Metals and Alloys Rep., 36 (1995), 123-129.
27) Y. Hoshizashi et al., "Dislocation in γ Channel in Single Crystal Ni-base Superalloy, CMSX-4, with Creep Deformation," 123rd Committee on Heat Resisting Metals and Alloys Rep., 36 (1995), 331-341.